



Alligator osteoderms: Mechanical behavior and hierarchical structure

Irene H. Chen^a, Wen Yang^{a,*}, Marc A. Meyers^{a,b}

^a Materials Science and Engineering Program, University of California, San Diego, La Jolla, CA 92093, USA

^b Departments of Mechanical and Aerospace Engineering and Nanoengineering, University of California, San Diego, La Jolla, CA 92093, USA



ARTICLE INFO

Article history:

Received 14 June 2013

Received in revised form 17 October 2013

Accepted 16 November 2013

Available online 1 December 2013

Keywords:

Alligator

Osteoderms

Scutes

Mechanical properties

Mechanisms

ABSTRACT

Osteoderms are bony scutes embedded underneath the dermal layers of the skin acting as a protection of the alligator (Archosauria: Crocodylia) internal organs and tissues. Additionally, these scutes function as an aid in temperature regulation. The scutes are inter-linked by fibrous connective tissue. They have properties similar to bone and thus have the necessary toughness to provide protection against predators. The scutes consist of hydroxyapatite and have a porosity of approximately 12%. They have a disc-like morphology with a ridge along the middle of the plate, called the keel; the outer perimeter of the disc has depressions, grooves, and jagged edges which anchor the collagen and act as sutures. Computerized tomography reveals the pattern of elongated pores, which emanate from the keel in a radial pattern. Micro-indentation measurements along the cross-section show a zigzag behavior due to the porosity. Compression results indicate that the axial direction is the strongest (UTS ~67 MPa) and toughest (11 MJ/m³); this is the orientation in which they undergo the largest external compression forces from predator teeth. Toughening mechanisms are identified through observation of the damage progression and interpreted in mechanistic terms. They are: flattening of pores, microcrack opening, and microcrack growth and coalescence. Collagen plays an essential role in toughening and plasticity by providing bridges that impede the opening of the cracks and prevent their growth.

© 2013 Elsevier B.V. All rights reserved.

1. Introduction

The existence of the crocodylians can be traced as far back as 180 million years ago, when they coexisted with dinosaurs [1]. They survived through volcanic eruptions, erratic climate changes, ice ages, and a possible asteroid collision with the earth at the Cretaceous-Tertiary boundary which occurred 65 million years ago, wiping out all but a few species. Alligators have to not only defend themselves from intra species predation but also contend with various predators. One of the important features that the alligators have evolved and developed through environmental and defensive selection is the “armored skin”. This characteristic was also found on dinosaurs and ancient fish [2]. The osteoderms on their dermis provide a protective barrier against attack, such as enemy's teeth and claws [3]. In ancient times, alligator osteoderms were used as army protective outfits; they were considered to be strong and tough enough to protect against arrows and blows from the enemy.

The alligator scutes are oriented along the back of the animal in the transverse direction with 15 rows of 6 larger plates (per row) and another 5 rows of 3 smaller plates near the posterior shown in Fig. 1a [4]. The scute (cross-sectional view in Fig. 1b and c), a round disc-like plate, has a varying diameter of 5 cm to 8 cm depending on the anatomical location along the back of the animal and on the animal's size. It has a keel, a tilted projection, in the middle of the disc. The keels arranged in rows give out the spiked characteristics in the back of the animal

(Fig. 1a). The keel is assumed to provide a structure which the skin can anchor itself on [6]. Other morphological characteristics include the small nutrient bony network on the surface near the keel. Viewing from the longitudinal direction (Fig. 1b) a porous region is revealed, similar to the structure of bovine bone. The osteoderms overlap [7] and are inter-connected by collagen fibers [8,9]. The limbs are also covered by osteoderms [10]. Due to the connection mechanisms, the entire alligator skin with osteoderms is very flexible [11]; especially, the axial and paraxial locomotor apparatus is quite mobile [10].

The formation of an alligator scute begins with calcium mineralization at the center (keel region) and proceeds radially, one year after hatching; calcium is gradually deposited on the collagen fibers from the surrounding dermis layer. Before calcification, the integument has already developed into the epidermis and dermis regions. Vascularization is seen throughout the dermis region. The individual osteodermal development is a synchronized process across the body sequenced by firstly forming dorsally next to the neck region and then gradually growing by the addition of successive elements along the caudal and lateral positions [12,13]. Growth marks [9,14] are formed, comprising annuli deposited in winter and zones formed in the summer. It was proposed that under palaeoenvironmental conditions, osteoderms might have provided calcium storage [15]. The osteoderms also provide other functionalities for alligators as suggested by Seidel [6]: thermal absorption and transformation. The osteoderms absorb radiant heat efficiently during basking and can rapidly transfer and carry heat from the outside surroundings due to their vascularity. The vascular network throughout the osteoderms controls the animal's body thermoregulation

* Corresponding author.

E-mail addresses: wey005@eng.ucsd.edu, wyang8207@gmail.com (W. Yang).

by vasoconstriction and vasodilation [6]. This helps with the body temperature regulation of the animal. The vascularization also allows the osteoderms to store calcium [16].

The osteoderms are bony plates and as such the known response of bone is essential to their understanding. Bone has an extraordinary toughness that is enabled by the toughening mechanisms that were identified by Ritchie *et al.* [17,18]. These toughening mechanisms are divided into intrinsic and extrinsic. The extrinsic toughening mechanisms act to shield the crack from the applied load and operate behind the crack front. Four extrinsic toughening mechanisms are present in bone: crack deflection, uncracked ligament bridging, collagen fibril crack bridging, and microcracking. Intrinsic mechanisms, on the other hand, typically act ahead of the crack tip and reduce stresses and strains through localized yielding and redistribution of stresses [19–22], or may even promote crack growth.

There is almost no information in the literature on the mechanical response of alligator osteoderms. An important goal of the research whose results are presented here was to establish the principal toughening mechanisms in the osteoderm. Since the osteoderm acts as a protection for the alligator, it is proposed that this study can inspire novel material designs, such as flexible armor.

2. Experimental procedure

The scutes in the present work are from American Alligators with age 8–10 years old. The water content of scutes was measured by drying them in a furnace for 4 h at 100 °C and weighing them before and after the treatment. The protein content was measured by heating the scute in furnace for 24 h at 400 °C. The alligator scutes were characterized using X-ray diffraction, optical microscopy, and scanning electron microscopy (SEM, Phillips XL30 SEM, Hillsboro, Oregon, USA). The mechanical behavior including the micro-hardness and compression response was examined to establish the fracture mechanisms and the relationship between the microstructure and mechanical behavior. The samples were kept in water because the osteoderm has a vascular network in the structure which indicates that blood flows

through it when the alligator is alive. All the samples were coated with iridium prior to SEM observation.

2.1. X-ray diffraction

X-ray diffraction (XRD) was performed on the powder collected from the alligator's osteoderm using a bench top XRD system (MiniFlex TM II, Rigaku Company, Austin, Texas). The scan was performed continuously from $2\theta = 0$ to 60° , with a step size of 0.01° at a rate of $1^\circ/\text{min}$. The radiation source was $\text{CuK}\alpha 1$ with a wavelength of 0.154 nm.

2.2. Micro-indentation

The alligator scutes were cut longitudinally and transversely to determine the Vickers hardness variation through the thickness. They were ground using 180#–2500# silicon carbide paper and then polished with 0.3 μm and 0.05 μm alumina powder to ensure smooth surfaces. Hardness tests were performed in dry condition under a relative humidity of ~78% using an indentation load of 100 g (holding time: 10s) with a LECOM-400-H1 hardness testing machine (LECO M-400-HI, Leco Co., Michigan, USA).

2.3. Compression tests

Due to the dimensional constraints on the alligator scutes, 30 samples were cut into cubes with approximately 5 mm \times 5 mm \times 5 mm. Before testing, they were immersed in fresh water for more than 24 h. Compression tests were conducted using a 30 kN load cell equipped universal testing system (Instron 3342, Norwood, MA) at a strain rate of 10^{-3} s^{-1} . Three loading orientations were adopted as shown in Fig. 1b and c; the axial direction (orientation A in Fig. 1b and c) is along the thickness of the scute, the longitudinal (orientation B in Fig. 1b and c) is along the keel of the scute, while the transverse (orientation C in Fig. 1b and c) is perpendicular to the keel. The compression samples were tested immediately after removal from the water. All

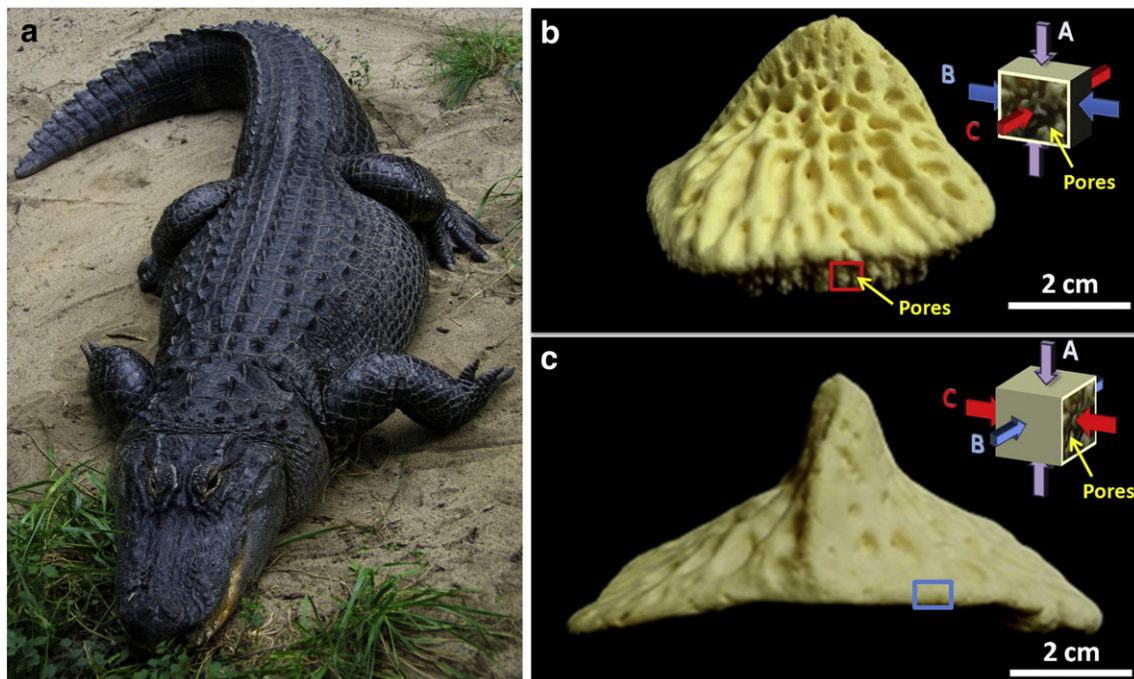


Fig. 1. (a) Alligator showing protrusions on back, each one corresponding to a scute [5], (b) longitudinal view of a scute, (c) transverse view of a scute; the schematics on the top right corners of (b) and (c) show the loading orientations of compression samples.

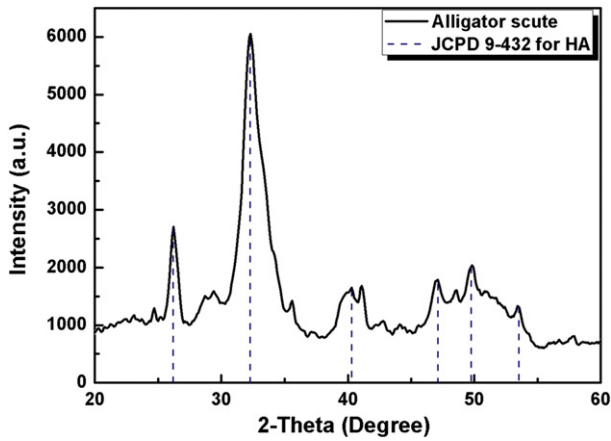


Fig. 2. X-ray diffraction of alligator scute; hydroxyapatite peaks marked by dashed lines (JCPD 9-432).

compression tests were performed at room temperature with ~78% humidity.

3. Results and discussion

3.1. Structural characterization

The wet alligator scute contains ~64.4 wt.% mineral, ~22.82 wt.% protein and ~12.78 wt.% water. Fig. 2 shows the XRD pattern of the alligator scute. The main mineral component is, according to JCPD file 9-432, hydroxyapatite (HAP).

Fig. 3 shows the micro-computed tomography (micro-CT) scan of an alligator scute with a keel in the middle. Around the keel, there is a

network of ridges with small round pits between them (Fig. 3a). The pores or channels in the alligator scute radiate from the center of the keel to the edges of the scute (Fig. 3b). Fig. 3c shows the transverse cross section (orientation B in Fig. 1b) perpendicular to the keel with smaller pores at the two sides of the keel; the longitudinal cross section along the keel (orientation C in Fig. 1b) reveals larger elongated pores, shown in Fig. 3d. The pores range from 20 μm to 150 μm . As is shown in Fig. 3, the sizes of the pores vary from inner (larger) to outer (smaller). The pores can be the destinations of the crack propagation and bring light weight to the structure. One scute contains ~12% porosity.

Along the transverse direction passing through center (Horizontal line in Fig. 3b), pores (rounded shapes) with diameters of 50 ~ 100 μm appear with a spacing of 200 ~ 500 μm , as shown in Fig. 4a. These round pores are surrounded by concentric lamellar ring layers (dashed circles in Fig. 4b). Along the longitudinal direction close to the keel (position marked in Fig. 4c), some pores are elongated; this indicates that these porous channels were not sectioned normally, but at a small angle. They have a length of 200 ~ 250 μm and a diameter of 50 ~ 100 μm radially from the keel. In addition to pores, tubules are also found in the structure near the keel. Along the thickness of the tubules, some ligaments or fibrils are found (Fig. 4d). These are collagen fibers that compose the bone together with hydroxyapatite.

The collagen hierarchical organization is shown in Fig. 5a. At the lowest spatial scale, one can observe the individual fibrils with a diameter of ~100 μm and a characteristic d spacing of approximately 67 nm. This dimension is shown in Fig. 5a. At a higher spatial level, one can identify two regions. The fibrils organize themselves into straight fibers with a diameter of ~50 μm (between the dashed lines shown in Fig. 5b). These fibers require channels in the structure. One such channel is shown in Fig. 5c (between the dashed lines). The fiber was pulled out of it during the fracture process. In other, adjoining regions, the collagen fibrils are less organized and more intermeshed with the HAP crystals. Such a region is shown in Fig. 5d. The net result of this

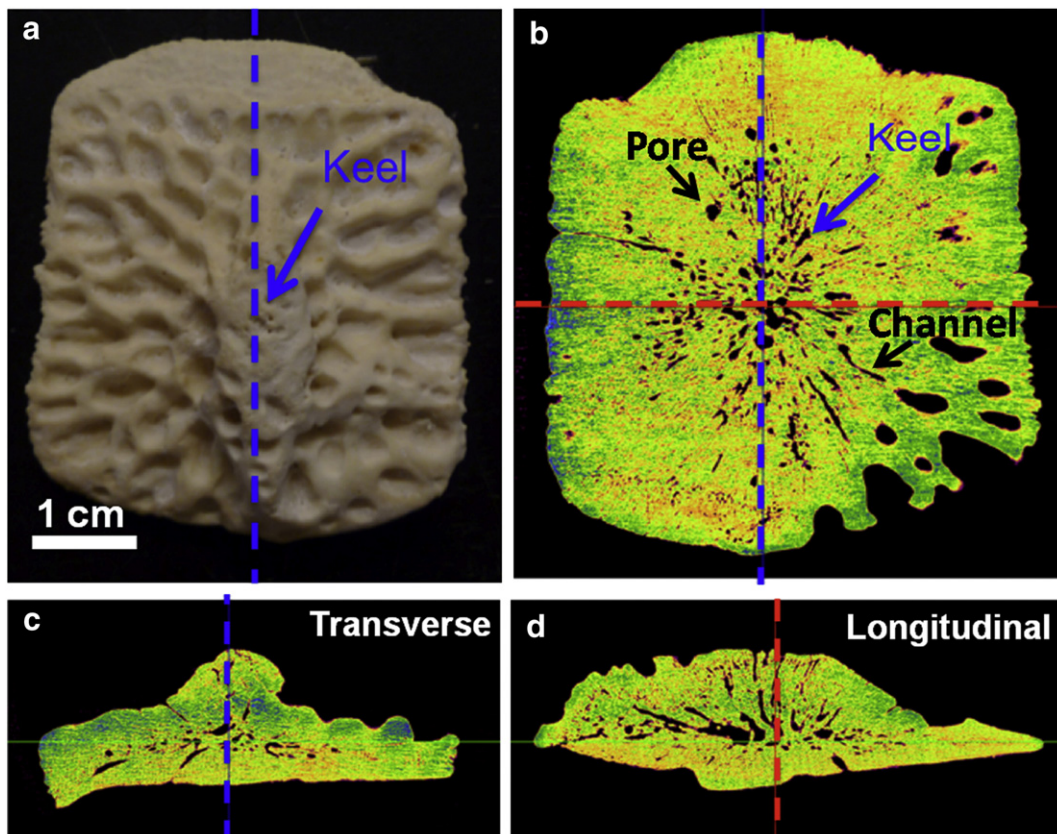


Fig. 3. (a) Scute in alligator osteoderm, (b) micro-CT on top view of scute, (c) micro-CT on the transverse view of the scute, (d) micro-CT on the longitudinal view of the scute.

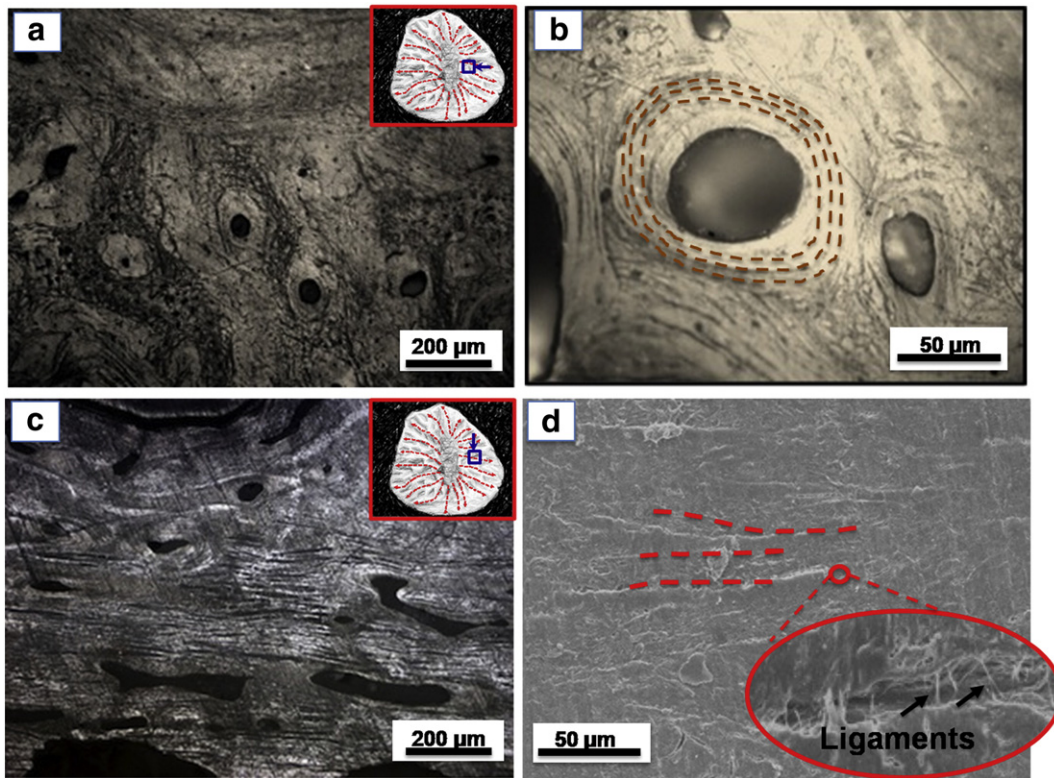


Fig. 4. (a) Transverse cross section showing the round pores, (b) round pores surrounded by rings of lamellae, (c) longitudinal direction showing elongated pores and channels; (d) ligaments in the little channels.

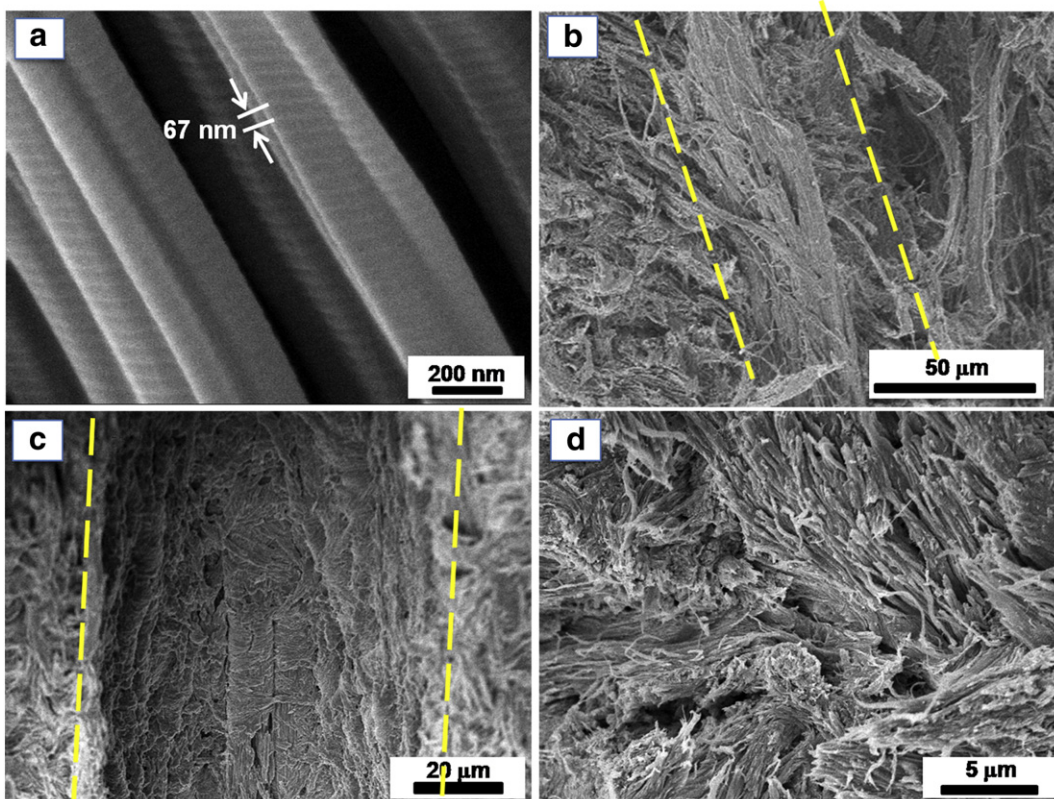


Fig. 5. (a) Collagen fibrils with the characteristic of 67 nm d spacing, (b) collagen fiber bundle with width of ~50 μm, (c) a channel with the diameter of ~50 μm, (d) structure of the matrix away from the fibers.

multiscale composite is an impressive toughness, as will be seen in Section 3.3.

3.2. Microhardness

Microhardness tests were conducted along the longitudinal cross section through the thickness of the alligator scute. Fig. 6 shows the microhardness variation from the interior to the exterior. The average size of these hardness samples along the thickness is 8 mm. To identify the results through the different thickness of the hardness samples, a normalized distance from exterior to interior (the distance from indentation position to the exterior surface divided by the overall thickness) was used to provide the position of the indentations on the samples shown in Fig. 6. At least three hardness measurements were made in each position across the thickness. The hardness across the whole thickness of the alligator scute shows a zig-zag pattern. This is due to the porous structure of alligator scute, indicated by the data in the ellipse in Fig. 6; the lowest hardness value is ~280 MPa, while the highest hardness can reach ~470 MPa. If an indentation interacts with a pore, the hardness is lower. As shown in Fig. 6, the size of the indent in the non-pore position is ~10 μm where it shows a higher hardness, however, the one close/in the pore position is much larger (~80 μm). The higher hardness values are comparable with the values for human cancellous bone of ~479 MPa [23].

3.3. Compression behavior

The compression tests were performed in three orientations using 6–10 samples for each. Band plots were made to represent the general information of compression behavior in the three orientations shown in Fig. 7. The compressive strength was obtained from the highest value before densification, and the modulus (E) was measured from the slope of the linear elastic deformation region shown by the representative solid stress–strain curve. The toughness is the area underneath the stress–strain curve up to fracture. Table 1 summarizes the average values of failure strength, modulus and toughness for each orientation. It is clear that the alligator scute has the highest compressive strength through the thickness direction (orientation A shown in Fig. 1b). The compression strength (40 ~ 70 MPa) is lower than one third of the hardness (300 ~ 450 MPa) on the surface because the compression sample contains an assembly of pores in the volume rather than on the surface of hardness sample. A bilinear behavior is observed for the three orientations, which indicates that the scutes undergo some “plasticity” upon loading. The “plasticity” is caused by the interaction

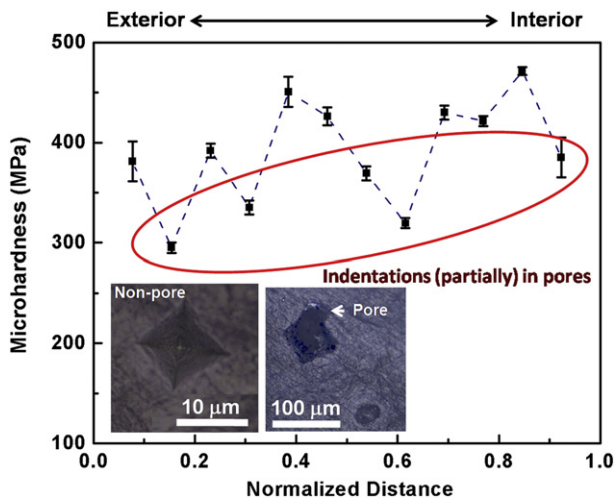


Fig. 6. Micro-hardness from interior to exterior (normalized distance) of the cross-section of alligator scute with the indentations in the compact (non-porous) region and porous region.

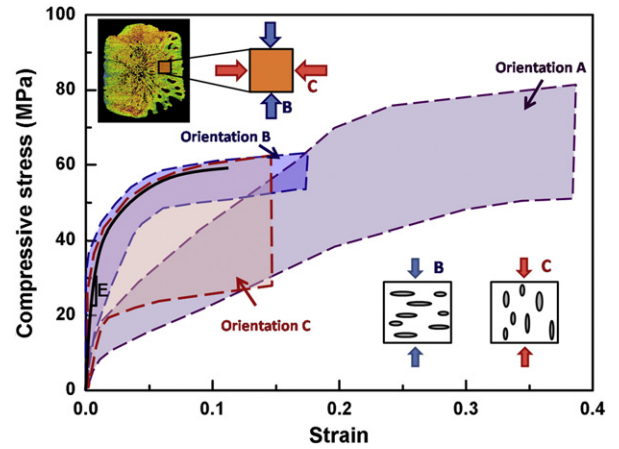


Fig. 7. Band plots of the compression tests in three orientations; schematic on the right bottom shows the orientations of loading; schematics on the left top show the structures in longitudinal (B) and transverse (C) orientations.

between the structural elements when subjected to compressive loading, such as fiber or ligament sliding or stretching and pore collapse. It is worth mentioning that the scutes have the highest value in strength and toughness along orientation A, which is the expected direction for the compression by predators' teeth. As the short axis of the elliptical pores in orientation B is along the compression direction, the pores were compressed and closed until full densification is reached. Hence, the elastic modulus of the scute in orientation B is higher and the band plot is thinner (more consistent). However, in orientation C, the loading direction is along the long axis of the elongated pores thus resulting in more irregular collapse of the pores as well as axial splitting; therefore, the strength and toughness are the lowest.

The strength of the scute in three orientations was analyzed using the Weibull method. Fig. 8 shows that at the 50% probability of failure, the stress in thickness direction (orientation A) is 67 MPa, higher than that of the other two orientations (58 MPa and 40 MPa) which is consistent with the band plots (Fig. 7). The Weibull modulus shows the variability of the data; the higher Weibull modulus, the less variability the data shows. The strengths in orientation B ($m = 13.6$) vary less because the elliptical pores with short axis aligned in the loading direction are readily collapsed in deformation with less axial splitting or crack opening in the structure.

In order to evaluate and understand the evolution of the mechanical response of the alligator scute under loading, compression tests were performed on the samples in orientation A by loading–unloading three times at prescribed strains (Fig. 9). The strain was calculated by measuring the specimen length after unloading. In the first loading cycle, the plot shows a modulus of ~1.5 GPa and then a decrease in slope that is indicative of “plasticity”. The differences in the stress–strain response between the two specimens in the first cycle are significant and can be attributed to the level of porosity. The elastic modulus is reduced to 0.5–0.6 GPa in the second loading cycle. The second cycle shows a most interesting response, indicative of “plasticity”. Upon unloading, there is no significant permanent deformation. This is attributed to the damage (formed in first cycle through microcracks) that is impeded from propagation. Microcracks are responsible for ‘plasticity’

Table 1
Compressive properties of alligator scute in three orientations.

	Orientation A (Axial)	Orientation B (Longitudinal)	Orientation C (Transverse)
Strength (MPa)	65.2 ± 9.2	57.2 ± 3.1	42.4 ± 13.3
Young's modulus (GPa)	2.2 ± 0.6	4.9 ± 3.1	5.7 ± 2.7
Toughness (MJ/m ³)	10.2 ± 3.0	6.0 ± 1.6	3.3 ± 2.2

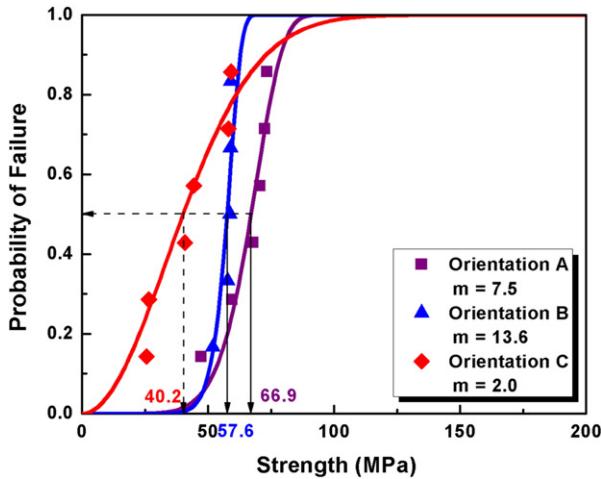


Fig. 8. Weibull plots of compressive strengths in orientations A, B, and C. Strengths at 0.5 failure probability marked in abscissa axis.

but the collagen fibers that form the bridges do not allow them to propagate. Thus, the cracks open upon loading and reclose upon unloading.

Eventually (cycle 3) this effect disappears and damage accumulation leads to failure. As more and more cracks are generated, the pores in the structure are gradually collapsed and the structure starts to split.

We used two regions on the lateral surfaces of the specimen to compare the damage: one adjacent to a pore and the other representative of the bulk. Fig. 10a, b shows the lateral surface of a specimen after 1st compression to $\sim 10\%$ strain and unloading. The loading direction is indicated by the arrows in the figure. The pore was $\sim 5\%$ flattened by the loading. A pattern of cracks is clearly seen. Around the void, cracks initiate at or close to the surface and propagate into the pores rather than contributing to the main failure of the scute. One can clearly see the greater number of cracks after a strain of 0.1. These additional cracks are marked by arrows. The crack sizes were measured in the squared areas (marked by the box) at the left bottom of the pore. The average size of the cracks increases from $15\ \mu\text{m}$ (1st compression) to $19\ \mu\text{m}$ (2nd compression). The other area (Fig. 10c and d) contains microcracks that form a network. After the second loading, the cracks were more open, but still connected by the collagen fibers (right bottom in

Fig. 10d). Since the cracks were not completely open, the sample did not collapse.

Fig. 11a and b shows the cracks around a pore generated by the axial loading. One main crack was initiated and started to propagate, as shown by the arrow in Fig. 11a. At the micrometer scale, mineral bridges with a width of $\sim 20\ \mu\text{m}$ appear along the crack (Fig. 11b). Ligaments (collagen fibers) are stretched across the crack, but still connect to both sides and form bridges (Fig. 11c). Finally the ligaments fracture and are misaligned (arrows in Fig. 11d) by the shear stresses. Stress concentrations are generated by the loading of a body with pores in the structure. The small cracks, which were generated around the pores, propagate into the pores rather than contributing to the main failure of the scute (Fig. 11b).

3.4. Toughening mechanisms

Fig. 12 summarizes the toughening mechanisms of the alligator scute under compressive loading. Firstly (Fig. 12a), cracks are generated parallel to the loading direction, especially at the top and bottom of the pores due to the tensile stress concentration. These cracks contribute to the decrease in the volume of the voids.

In the bulk (Fig. 12b), cracks are also generated but impeded from growth by the bridging collagen fibers in the structure, thus avoiding the complete splitting and thereby extending the plastic regime of bone. As the collagen fibers exhibit significant elasticity, the axial splitting with collagen fibers bridges provides an elastic response and inhibits “plasticity”.

As the loading proceeds (Fig. 12c), cracks continue to propagate, and the mineral bridges are formed.

Three mechanisms—flattening of pores, microcrack opening, and microcrack growth and coalescence—operate together to provide toughness to the bone in scutes. Collagen plays an essential role in the toughening by providing bridges that impede the opening of the cracks, thus preventing their growth.

4. Conclusions

Crocodylia have survived through hundreds of millions of years and have developed an effective flexible dermal armor. Besides thermal absorption and transformation, the osteoderms also provide important protection to the alligator without sacrificing flexibility. In this study, we focused on the relationship between the structure and mechanical behavior of the alligator scute (one unit of the osteoderm). Each scute

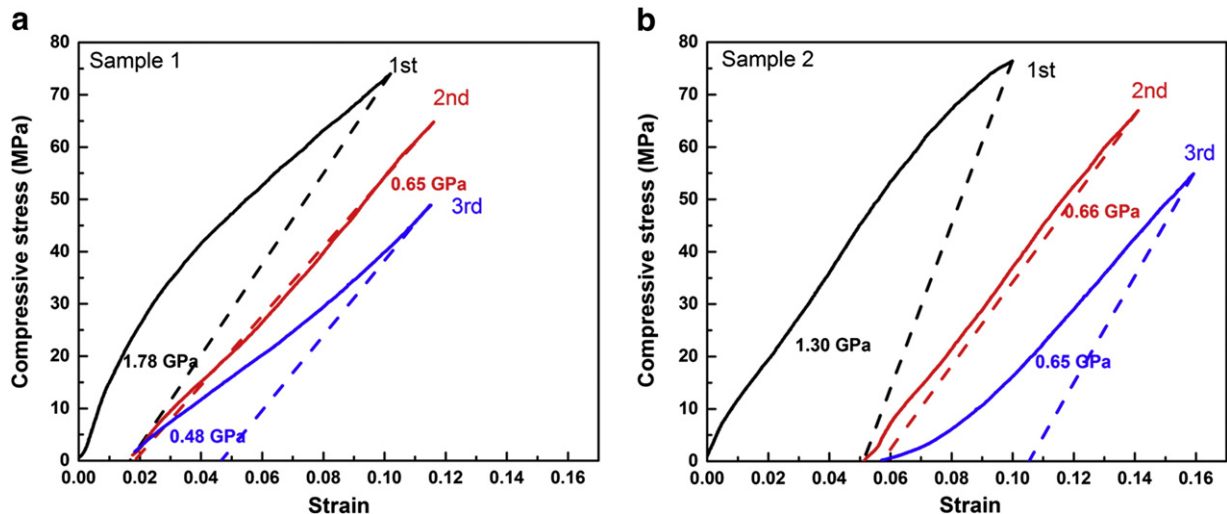


Fig. 9. Compression results (three loading-unloading cycles) of wet scutes tested in orientation A. The elastic modulus is significantly reduced from $\sim 1.5\ \text{GPa}$ to $0.4\text{--}0.6\ \text{GPa}$ due to damage accumulation in the specimen during loading cycles.

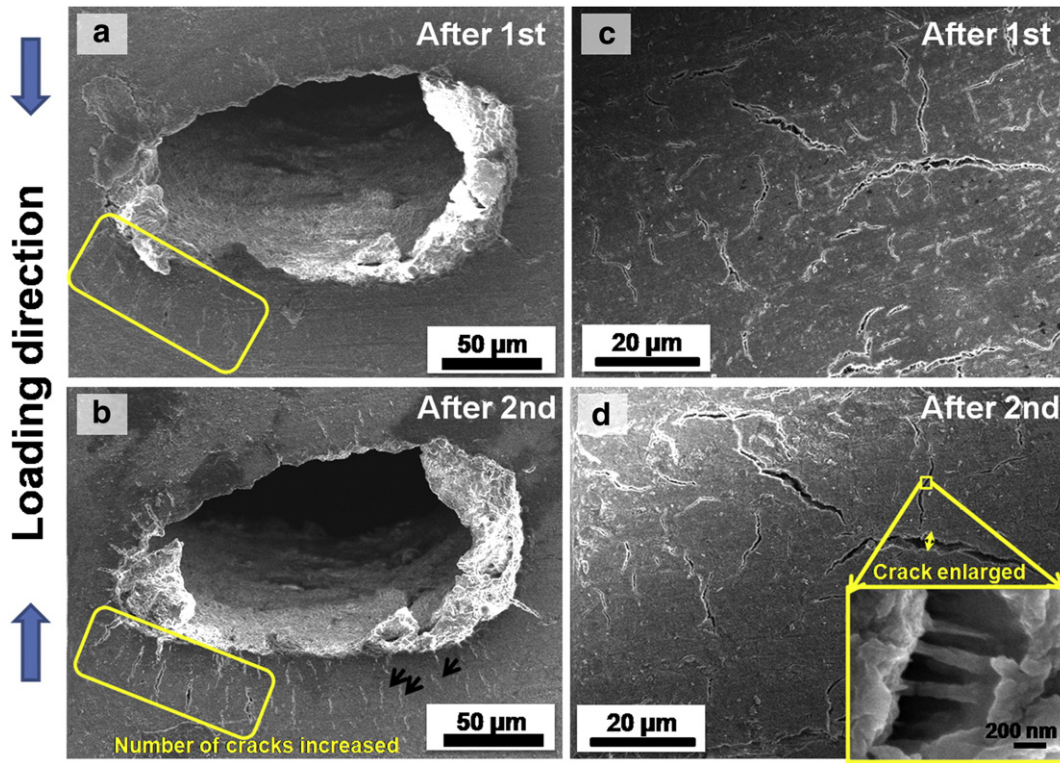


Fig. 10. Structure characterization of the sample after (a) and (c) 1st and (b) and (d) 2nd loading. The concentration of cracks increases; the cracks are opened by the loading but are prevented from propagation by the collagen bridges.

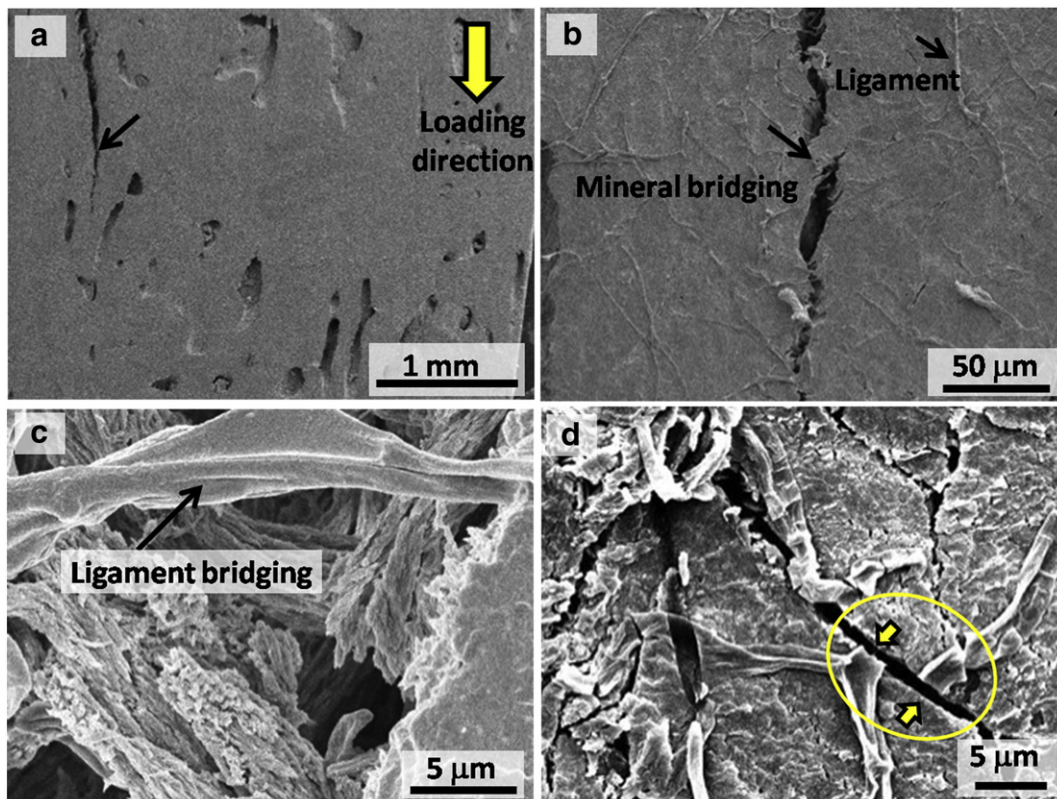


Fig. 11. (a) Overall of sample after compression showing axial splitting along the loading direction; (b) mineral bridges; (c) stretched mineralized collagen fiber inside crack; (d) fractured and misaligned collagen ligament.

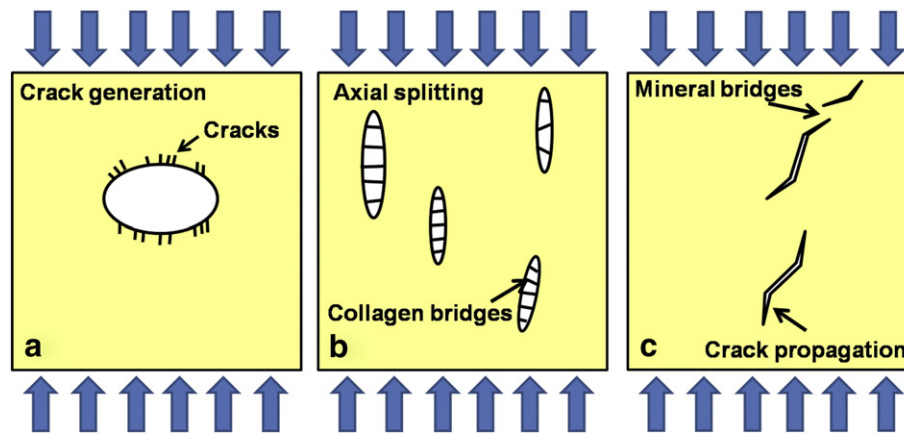


Fig. 12. Schematic drawing of the principal toughening mechanisms acting in the osteoderm; (a): crack generation close to the pores promoting their closure, (b) microcrack opening and formation of collagen bridging, and (c) microcrack growth, coalescence, and mineral bridges.

has a keel in the middle and many ridges around it, forming a network structure on the surface. The main conclusions are emphasized as the following:

1. The alligator scute, which is a bone containing hydroxyapatite and collagen, has a porous structure with features including ligaments and fibers. The porous structure decreases the weight of the osteoderm, ensuring mobility to the alligator. The matrix around the pores has a high hardness ensuring that the osteoderm can resist penetration by teeth and claws.
2. The bilinear stress–strain curve indicates a pseudo-plastic response of the alligator scute under compressive loading. The reloading response does not have the same Young's modulus as the original loading curve, due to the damage to the structure in the form of cracks. The scutes can absorb more energy in the thickness direction, which is the orientation in which the teeth of a predator would impinge. The loading–unloading and reloading responses of the scute show that after the first loading, there is still significant ability for the structure to reload.
3. Three principal toughening mechanisms were identified: flattening of pores, collagen bridges impeding growth of cracks, and formation of mineral bridges. These mechanisms contribute to energy dissipation and toughness upon loading. These mechanisms have been identified by Vashishth et al. [19–22] and Ritchie et al. [17,18] for different types of bone.

Acknowledgments

This research was partially funded by the National Science Foundation (Grant Number: DMR-1006931) and by the UC Labs Program (Grant number: 12-LR-239079). We appreciate Dale Ceballos (Creative-Aztec) for his valuable information on the alligator osteoderms. We thank Prof. G. Arhenius for the use of his X-ray diffractometer. Discussions with Dr. P.-Y. Chen are gratefully acknowledged.

References

- [1] W.T. Neil, *The Last of the Ruling Reptiles: Alligators, Crocodiles and Their Kingdom*, Columbia University Press, New York and London, 1971.
- [2] M.A. Meyers, Y.S. Lin, E.A. Olevsky, P.-Y. Chen, *Battle in the Amazon: Arapaima versus Piranha*, *Adv. Mater.* 14 (2012) 279–288.
- [3] S. Grenard, *Handbook of Alligators and Crocodiles*, Krieger Publishing Company, Malaba, 1991.
- [4] D. Schwarz-Wings, E. Frey, T. Martin, Reconstruction of the bracing system of the trunk and tail in hyposaurine dyrosaurids (Crocodylomorpha; Mesoeucrocodylia), *J. Vertebr. Paleontol.* 29 (2009) 453–472.
- [5] http://en.wikipedia.org/wiki/File:American_Alligator.jpg.
- [6] M.R. Seidel, The osteoderms of the American Alligator and their functional significance, *J. Herpetol.* 35 (1979) 375–380.
- [7] T.E. Williamson, *Brachychampsia sealeyi*, sp. nov., (Crocodylia, Alligatoroidea) from the Upper Cretaceous (lower Campanian) Menefee Formation, Northwestern New Mexico, *J. Vertebr. Paleontol.* 16 (1996) 421–431.
- [8] I.A. Cerda, J.B. Desojo, Dermal armour histology of aetosaurs (Archosauria: Pseudosuchia), from the Upper Triassic of Argentina and Brazil, *Lethaia* 44 (2011) 417–428.
- [9] T.M. Scheyer, J.B. Desojo, Palaeohistology and external microanatomy of rauisuchian osteoderms (Archosauria: Pseudosuchia), *Palaeontology* 54 (2011) 1289–1302.
- [10] R. Hill, Osteoderms of *Simosuchus clarki* (Crocodyliformes: Notosuchia) from the Late Cretaceous of Madagascar, *J. Vertebr. Paleontol.* 30 (2010) 154–176.
- [11] W. Yang, I.H. Chen, B. Gludovatz, E.A. Zimmermann, R.O. Ritchie, M.A. Meyers, Natural flexible dermal armor, *Adv. Mater.* 25 (2013) 31–48.
- [12] M. Vickaryous, B.K. Hall, Development of dermal skeleton in Alligator mississippiensis (Archosauria, Crocodylia) with comments on the homology of osteoderms, *J. Morphol.* 269 (2008) 398–422.
- [13] L. Alibardi, M.B. Thompson, Scale morphogenesis and ultrastructure of dermis during embryonic development in the alligator (*Alligator mississippiensis*, Crocodylia, Reptilia), *J. Acta Zool.* 81 (2000) 325–338.
- [14] A.D. Tucker, Validation of skeletochronology to determine age of freshwater crocodiles (*Crocodylus johnstoni*), *Mar. Freshwater Res.* 48 (35) 343–351.
- [15] K.C. Rogers, M. D'Emic, R. Rogers, M. Vickaryous, A. Cagan, Sauropod dinosaur osteoderms from the Late Cretaceous of Madagascar, *J. Nat. Commun.* 564 (2011) 1–5.
- [16] J. Farlow, S. Hyashi, G. Tattersall, Internal vascularity of the dermal plates of *Stegosaurus* (Ornithischia, Thyreophora), *Swiss J. Geosci.* 103 (2010) 173–185.
- [17] R.O. Ritchie, Mechanisms of fatigue-crack propagation in ductile and brittle solids, *Int. J. Fract.* 100 (1999) 55–83.
- [18] R.O. Ritchie, M.J. Buehler, P.K. Hansma, Plasticity and toughness in bone, *Phys. Today* 62 (2009) 41–47.
- [19] D. Vashishth, J.C. Behiri, W. Bonfield, Crack growth resistance in cortical bone: concept of microcrack toughening, *J. Biomech.* 10 (1997) 763–769.
- [20] D. Vashishth, K.E. Tanner, W. Bonfield, Contribution, development and morphology of microcracking in cortical bone during crack propagation, *J. Biomech.* 33 (2000) 1169–1174.
- [21] D. Vashishth, K.E. Tanner, W. Bonfield, Experimental validation of a microcracking-based toughening mechanism for cortical bone, *J. Biomech.* 36 (2003) 121–124.
- [22] D. Vashishth, Rising crack-growth-resistance behavior in cortical bone: implication for toughness measurements, *J. Biomech.* 37 (2004) 943–946.
- [23] G. Boivin, Y. Bala, A. Doublier, D. Farlay, L.G. Ste-Marie, P.J. Meunier, P.D. Delmas, The role of mineralization and organic matrix in the microhardness of bone tissue from controls and osteoporotic patients, *J. Bone* 43 (2008) 532–538.